

# A new SCAO control concept based on mechanical mirror modes for METIS

Philip L. Neureuther<sup>a,b</sup> and Thomas Bertram<sup>b</sup> and Oliver Sawodny<sup>a</sup>

<sup>a</sup> Institute for System Dynamics, University of Stuttgart, Waldburgstraße 17/19,  
Stuttgart, Germany

<sup>b</sup> Max Planck Institute for Astronomy, Königsstuhl 17, Heidelberg, Germany

## ABSTRACT

The Mid-infrared ELT Imager and Spectrograph (METIS) enables high-resolution spectroscopic and coronagraphic imaging. To achieve diffraction-limited measurements, a single conjugate adaptive optics (SCAO) system comprising the ELT's deformable mirror M4, the ELT's tip-tilt mirror M5 and a pyramid wavefront sensor is used. Due to the large dimensions of the active mirrors M4 and M5, their temporal dynamics affect the METIS-SCAO control loop and its performance, thus rendering the design of suitable SCAO controllers difficult. We present a new model-based control concept for the METIS-SCAO system based on the mechanical modes of the active mirrors. This control concept offers several advantages, such as: the tip- and tilt-correction is split between M4 and M5 based on the different mirror dynamics; the controller can be easily reconfigured to compensate faulty M4-actuators; the controller can be easily extended to include additional features. An end-to-end simulation utilizing the presented control concept shows that it corrects the wavefront error well for the METIS-SCAO system configuration.

**Keywords:** Single Conjugated Adaptive Optics, AO Control Concept, METIS

## 1. INTRODUCTION

The Extremely Large Telescope (ELT) is currently under construction in the Atacama desert in Chile. By featuring a primary mirror of 39 m in diameter, it will be the largest ground-based telescope. Among the three first light instruments of the ELT, the Mid-infrared ELT Imager and Spectrograph (METIS) enables high-resolution spectroscopic and coronagraphic imaging. To obtain diffraction-limited measurements despite atmospheric and wind induced wavefront disturbances, METIS uses a single conjugate adaptive optics (SCAO) system. The METIS-SCAO system consists of the ELT's deformable mirror (DM) M4, the ELT's tip-tilt mirror (TTM) M5, an infrared pyramid wavefront sensor, and a SCAO controller implemented on a real time computer.<sup>1,2</sup>

The mirror M4 can adopt deformations with small amplitudes and high spatial frequencies and also features a fast temporal dynamics. In contrast, M5 provides large tip-tilt strokes with slow dynamics. Therefore, both active mirrors M4 and M5 can redundantly correct tip-tilt wavefront errors and the SCAO system is a dual-stage system (also referred to as tweeter woofer system). Furthermore, M4 and M5 are controlled by local control systems (LCS) ensuring their correct positioning.<sup>3,4</sup> Due to the large dimensions of the active mirrors and despite their LCS, the closed-loop dynamics of M4 and M5 cannot be neglected and affect the SCAO control loop and its performance. In order to achieve the best possible wavefront correction in this complex system configuration, we present a new model-based SCAO control concept based on the mechanical modes of the active mirrors M4 and M5.

Many different model-based and non-model-based AO control concepts have been described, tested and used on-sky since the first AO systems were developed for astronomic telescopes. Therefore, we will only report the most important results on dual-stage or similar systems. Conan et al.<sup>5</sup> derived a standard integral controller whose command matrix artificially separates the corrections of the active mirrors. Kulcsár et al.<sup>6</sup> presented a linear-quadratic-Gaussian (LQG) controller splitting the wavefront correction between a DM and a TTM, taking into account stroke limitations via a regularization term and neglecting the temporal mirror dynamics. Correira

---

Corresponding author: Philip L. Neureuther, e-mail: philip.neureuther@isys.uni-stuttgart.de

et al.<sup>7,8</sup> introduced several LQG controllers, each taking into account the temporal dynamics of the TTM but also neglecting the dynamics of the DM. Lavigne and Véran<sup>9</sup> proposed a control concept where the controller is evaluated in the spatial Fourier space and the control signal is split between the two active mirrors based on its spatial frequency. Sedghi et al.<sup>10</sup> presented a master-slave like control using two integral controllers to eliminate tip-tilt errors via a DM and a TTM. Gavel and Norton<sup>11</sup> described a controller that bleeds off corrections from the fast to the slow active mirror and uses modes obtained by a singular value decomposition (SVD) of the mirror influence functions. Perez et al.<sup>12</sup> proposed an adaptive modal controller utilizing modes similar to those of Gavel and Norton.<sup>11</sup>

The main *contribution* of this paper is the presentation of a new model-based SCAO control concept relying on the mechanical modes of the active mirrors M4 and M5 for METIS (see Fig. 3). This control concept is characterized in particular by the following:

- The wavefront error is split between the active mirrors M4 and M5 based on their temporal dynamics and provided spatial wavefront corrections (cf. single controller with command split<sup>5,9</sup>).
- The M4 and M5 controllers are decoupled and rely on the natural modes of the active mirrors exclusively defined by their mechanics (cf. coupled mirror controllers<sup>10-12</sup>, synthetic mirror modes<sup>5,11,12</sup>).
- The temporal and spatial dynamics of M4 *and* M5 are taken into account (cf. neglected temporal mirror dynamics<sup>6-8</sup>).

This paper is organized as follows: Section 2 establishes the most important basics of M4 and M5 as well as the modal transform. Subsequently, in Section 3, the proposed SCAO control concept is described and its benefits are highlighted. Section 4 shows results of an end-to-end simulation utilizing the proposed control concept. At the end, Section 5 summarizes the presented contents and provides possible directions for future work.

## 2. THEORETIC BASICS

In this section we introduce the most important characteristics of M4 (see Section 2.1) and M5 (see Section 2.2) affecting the design of the METIS-SCAO control system. Following this, we briefly establish the relevant essentials of the modal transform (see Section 2.3).

### 2.1 Deformable Mirror M4

The deformable mirror M4 (see Fig. 1a)<sup>2,3</sup>

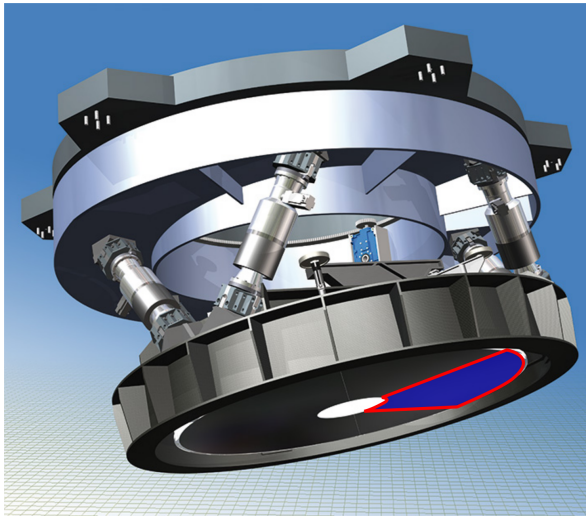
- can adopt deformations with small amplitudes and high spatial frequencies,
- features a fast temporal dynamics (see Eq. (1)),
- is flat and composed of six identical plate segments,
- has an inner diameter of  $\approx 0.5$  m and an outer diameter of  $\approx 2.5$  m,
- is controlled by an LCS ensuring its desired shape.

Each M4 segment plate is 1.95 mm thick, deformed by  $\approx 900$  actuators and elastically supported on its outer radial edge whereas all remaining edges are free (see Fig. 1b). The actuators of each segment are positioned in a triangular grid and are spaced  $\approx 31$  mm apart.

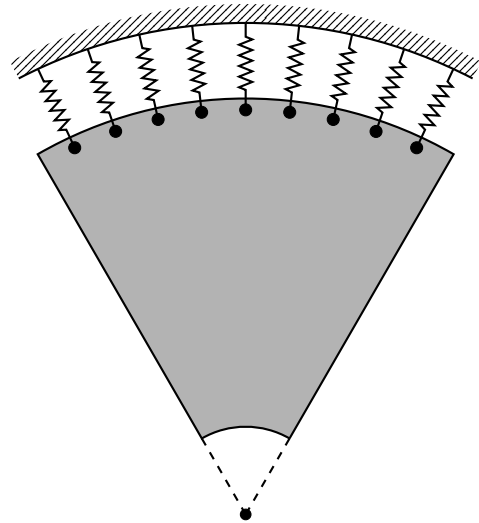
Using plate theory, the temporal *and* spatial dynamics of the M4 segments can be modeled as Kirchhoff-Love or Mindlin-Reissner plates, for example. Based on a plate-theoretical partial differential equation (PDE) model, the mechanical modes of the M4 segments can be determined. These modes depend exclusively on the segment geometry and its boundary conditions. Figure 2 shows the first six mechanical modes of the M4 segments derived from a simplified finite element model of M4 and sorted by their natural frequencies. The detailed modeling and modal analysis of the segments will be studied in future publications.

The temporal dynamics of M4, representing the association of the M4 control command  $U_{M4}(s)$  and its shape  $Y_{M4}(s)$ , is determined by the underlying M4-LCS. According to the specifications of the European Southern Observatory (ESO), we currently expect that this dynamics can be described as a second-order system

$$Y_{M4}(s) = \frac{\omega^2}{s^2 + 2\eta\omega s + \omega^2} e^{-T_a s} U_{M4}(s), \quad (1)$$



(a)



(b)

Figure 1: The deformable mirror M4. (a): Rendering of M4.<sup>13</sup> One of the six plate segments is highlighted. (b): Sketch of an M4 segment. The outer radial edge is elastically supported by springs whereas all remaining edges are free.

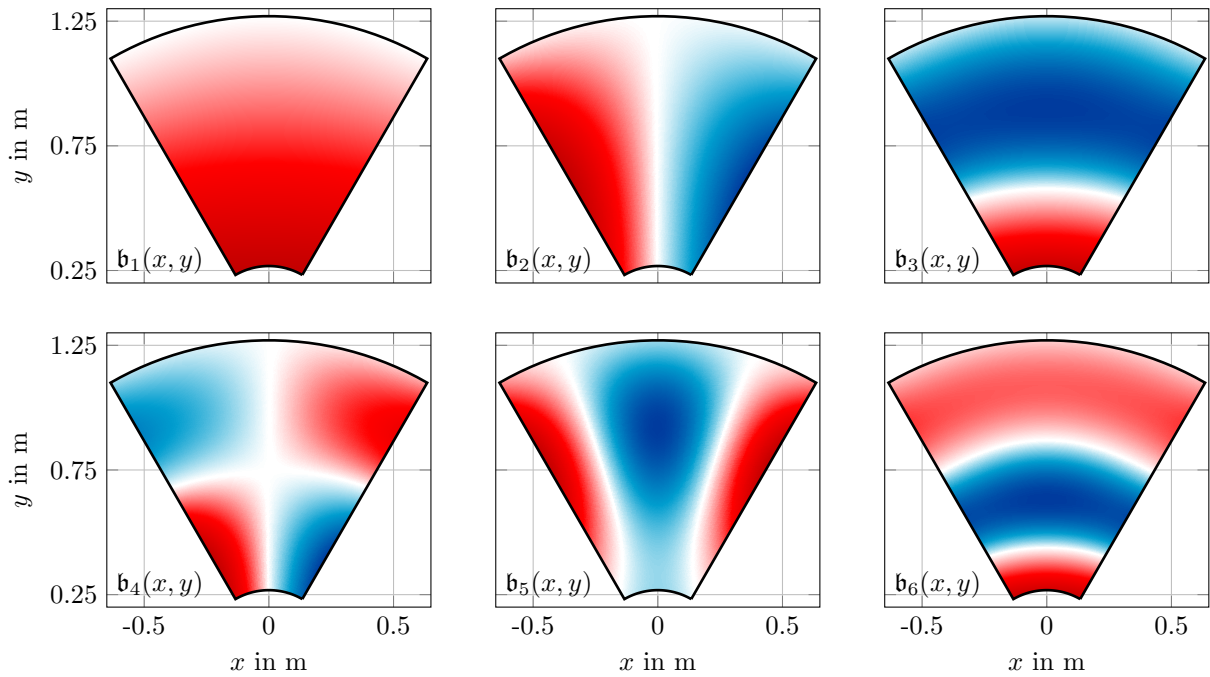


Figure 2: The first six mechanical modes  $\mathbf{b}_k$  of the M4 segments (sorted by their natural frequencies). Positive deflections are displayed in red, zero deflections in white, and negative deflections in blue.

with an angular frequency  $\omega \approx 2950 \frac{\text{rad}}{\text{s}}$ , a damping factor  $\eta \approx 0.65$ , and a time delay  $T_d \approx 1$  ms. Because the temporal dynamics of the mechanical M4 modes are significantly influenced by the M4-LCS and Eq. (1) shall apply to arbitrary mirror shapes, we assume that the dynamics of *all* M4 modes are (approximately) represented by Eq. (1). Furthermore, the mechanical modes are therefore considered as nearly decoupled.

## 2.2 Tip-Tilt Mirror M5

The tip-tilt mirror M5<sup>2,4</sup>

- size is  $\approx 2.2 \text{ m} \times 2.7 \text{ m}$ ,
- provides large tip-tilt strokes,
- features a slow temporal dynamics (see Eq. (2)),
- is flat and actuated by three piezo-electric drives,
- is controlled by a LCS ensuring the desired tip and tilt.

Like M4, the temporal dynamics of M5, representing the association of the M5 control command  $U_{M5}(s)$  and its tip-tilt  $Y_{M5}(s)$ , is determined by the underlying M5-LCS. According to the specifications of ESO, we currently expect that this dynamics can be described as a first-order system<sup>4</sup>

$$Y_{M5}(s) = \frac{\omega}{s + \omega} e^{-T_d s} U_{M5}(s), \quad (2)$$

with an angular frequency  $\omega \approx 63 \frac{\text{rad}}{\text{s}}$  and a time delay  $T_d \approx 1$  ms.

Furthermore, the spatial *and* temporal dynamics of the M5 mirror plate can be modeled via a PDE, enabling the determination of its mechanical modes. Since the LCS actively damps the mechanical modes of the M5 mirror plate,<sup>4</sup> exclusively tip and tilt are the relevant modes of M5 from the METIS-SCAO system's perspective.

## 2.3 Modal Transform

For distributed parameter systems, the modal transform is a common technique to reduce models and synthesize controllers.<sup>14</sup> Using the modal transform, a temporal and spatial PDE can be transformed into set of temporal ordinary differential equations (ODEs) which are easier to study and control.

We will briefly introduce the basics of the modal transform using a time-dependent function  $f(x, y, t)$  (e.g. deformation of a plate) with two spatial coordinates  $x$  and  $y$ . Let  $\mathcal{D} \subset \mathbb{R}^2$  be the spatial domain of  $f : \mathcal{D} \times \mathbb{R}_{>0} \rightarrow \mathbb{R}$ . Furthermore, let  $\mathbf{b}_k : \mathcal{D} \rightarrow \mathbb{R}$  be one of  $m$  basis functions resp. modes (e.g. modes of a plate, see Fig. 2). The time-dependent modal coefficient  $\mathbf{f}_k : \mathbb{R}_{>0} \rightarrow \mathbb{R}$  of the mode  $\mathbf{b}_k$  can be computed using the modal transform

$$\mathbf{f}_k(t) = \iint_{\mathcal{D}} \mathbf{b}_k(x, y) f(x, y, t) dx dy. \quad (3)$$

By means of the inverse modal transform

$$f(x, y, t) \approx \sum_{k=1}^m \mathbf{b}_k(x, y) \mathbf{f}_k(t), \quad (4)$$

$f(x, y, t)$  can be reconstructed approximately. The inverse transform for a set of points  $(x_n, y_n) \in \mathcal{D}$  can be written as the following matrix vector multiplication

$$\begin{pmatrix} f(x_1, y_1, t) \\ f(x_2, y_2, t) \\ f(x_3, y_3, t) \\ \vdots \end{pmatrix} \approx \begin{pmatrix} \mathbf{b}_1(x_1, y_1) & \mathbf{b}_2(x_1, y_1) & \mathbf{b}_3(x_1, y_1) & \cdots \\ \mathbf{b}_1(x_2, y_2) & \mathbf{b}_2(x_2, y_2) & \mathbf{b}_3(x_2, y_2) & \cdots \\ \mathbf{b}_1(x_3, y_3) & \mathbf{b}_2(x_3, y_3) & \mathbf{b}_3(x_3, y_3) & \cdots \\ \vdots & \vdots & \vdots & \ddots \end{pmatrix} \begin{pmatrix} \mathbf{f}_1(t) \\ \mathbf{f}_2(t) \\ \mathbf{f}_3(t) \\ \vdots \end{pmatrix}. \quad (5)$$

Usually the difference between the two sides of Eq. (4) decreases when the number of modes  $m$  increases.

### 3. MODAL CONTROL

The METIS-SCAO system features the following characteristics complicating the development of a suitable control concept: The SCAO system is a dual-stage system with the active mirrors M5 (large strokes, slow dynamics) and M4 (small strokes, fast dynamics). Therefore, the tip and tilt correction has to be split appropriately between M4 and M5 especially to achieve a good wavefront correction under poor observation conditions. Furthermore, the temporal dynamics of the mirrors M4 *and* M5 controlled by their respective LCS (see Eq. (1) and (2)) cannot be neglected when operating the SCAO system at a loop frequency of 1 kHz. Moreover, M4 shows a coupled spatial and temporal dynamics.

In the following section, we present a modal and model-based control concept for the METIS-SCAO system dealing with its features (see Section 3.1). Subsequently we briefly describe the realization (see Section 3.2) and highlight the benefits (see Section 3.3) of the proposed concept.

#### 3.1 Control Concept

Taking into account the characteristics of the METIS-SCAO system, the basic idea for the presented control concept is: The temporal low-frequency tip-tilt component of the wavefront error is corrected by M5 and the “remaining” wavefront error by M4. Furthermore, two *independent* controllers command the active mirrors M4 and M5 according to the wavefront errors “assigned” to each of them. Additionally, both mirror controllers rely on the respective mechanical modes of M4 (i.e. mechanical modes of the M4 segment plate, see Section 2.1) and M5 (i.e. tip and tilt, see Section 2.2).

The presented control concept is depicted in Fig. 3 and works as follows:

1. Extraction of the tip-tilt wavefront error  $\epsilon_{tt}$  out of the wavefront error  $e_{wf}$  (cf. tip-tilt calculation)
2. Temporal frequency split of the tip-tilt wavefront error  $\epsilon_{tt}$  into a high-frequency component  $\epsilon_{tt,hf}$  and a low-frequency component  $\epsilon_{tt,lf}$  (cf. crossover network)
3. Evaluation of the modal M5 controller:
  - I) Transformation of the low-frequency tip-tilt component  $\epsilon_{tt,lf}$  into the M5 coordinate system (cf.  $\mathcal{T}_{M5}$ )
  - II) Computation of the tip-tilt commands for M5 (cf. M5 controller)
  - III) Transformation of the M5 tip-tilt commands into the M5 actuator commands  $u_{M5}$  (cf.  $\tilde{\mathcal{T}}_{M5}$ )
4. Evaluation of the modal M4 controller:
  - I) Calculation of the wavefront error  $\epsilon_{M4}$  without the low-frequency tip-tilt component  $\epsilon_{tt,lf}$  in the mechanical mode basis of M4 (cf.  $\mathcal{T}_{M4}$ )
  - II) Computation of the modal commands for M4 (cf. M4 controller)
  - III) Transformation of the modal M4 commands into the M4 actuator commands  $u_{M4}$  (cf.  $\tilde{\mathcal{T}}_{M4}$ )

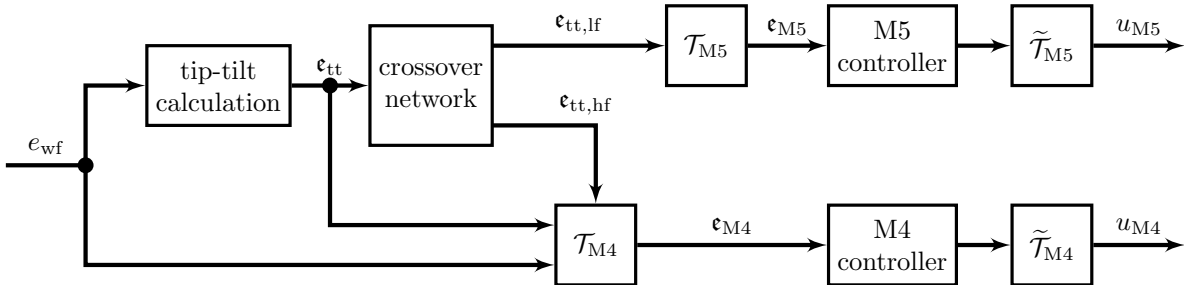


Figure 3: The SCAO control concept based on mechanical mirror modes. The wavefront error is split up into a low-frequency tip-tilt and a residual component. These error components are corrected by M5 and M4 respectively.

#### 3.2 Realization

Table 1 describes how to realize the components of the presented SCAO control concept (see Fig. 3) in principle. The exact implementation of the crossover network and the M4/M5 controllers are design parameters and significantly influence the performance of the SCAO system. In the future, we investigate which crossover networks and M4/M5 controllers provide the best wavefront correction for METIS.

Table 1: Principal realization of the presented SCAO control concept (see Fig. 3).

component	realization
tip-tilt calculation	linear regression of tip and tilt
crossover network	high-pass and low-pass filters (e. g. Butterworth or Linkwitz-Riley filters)
$\mathcal{T}_{M5}$	matrix vector multiplication
$\mathcal{T}_{M4}$	Vector based calculation: $\mathbf{e}_{M4}(t) = {}_{M4}\mathcal{M}_{wf} e_{wf}(t) + {}_{M4}\mathcal{M}_{tt} (\mathbf{e}_{tt,hf}(t) - \mathbf{e}_{tt}(t))$ ${}_{M4}\mathcal{M}_{\bullet}$ : matrix to transform an signal into the mechanical mode basis of M4
M5 controller	controller relying on tip and tilt of M5 (if necessary including a observer)
M4 controller	controller relying on the mechanical mode basis of M4 (if necessary including a observer)
$\tilde{\mathcal{T}}_{M5}$	matrix vector multiplication (inverse modal transform, see Eq. (5))
$\tilde{\mathcal{T}}_{M4}$	matrix vector multiplication (inverse modal transform, see Eq. (5))

### 3.3 Benefits

The most important benefits of the presented modal and model-based control concept for the METIS-SCAO system (see Fig. 3) are:

- The distribution of the tip-tilt correction between the DM (M4) and the TTM (M5) is based on the mirrors' dynamics and is computationally cheap. Furthermore, M4 is correcting nearly no low-frequency tip-tilt wavefront errors, saving actuator stroke for poor observation conditions.
- The concept can be easily reconfigured to compensate for faulty M4 actuators by adapting the inverse modal transform  $\tilde{\mathcal{T}}_{M4}$  (see Eq. (5)).
- The M4 and M5 controllers can be designed independently and fully customized to the respective active mirror.
- The concept can be easily extended to include additional features (e. g. offloading in case of actuator stroke saturation).

## 4. SIMULATION RESULTS

In order to demonstrate that the presented modal and model-based control concept (see Section 3.1) is well suited for the METIS-SCAO system, we performed an end-to-end simulation utilizing this concept and ELT-like observation conditions. We will first introduce the precise setup of the end-to-end simulation (see Section 4.1) and then discuss the obtained results (see Section 4.2).

### 4.1 Setup

Table 2 shows all essential configuration parameters of the end-to-end simulation utilizing the presented control concept. Note that the inverse modal transforms  $\tilde{\mathcal{T}}_{M4/M5}$  are omitted in this simulation, since both active mirrors M4 and M5 are represented via their respective modes. Moreover, the simulation was performed in a modified version of the AO simulation-tool COMPASS.<sup>15,16</sup>

In this simulation, the crossover network is realized via modified Linkwitz-Riley low-pass and high-pass filters.<sup>17</sup> The transfer function of the crossover filters are

$$\frac{\mathcal{L}\{\mathbf{e}_{tt,lf}(t)\}}{\mathcal{L}\{\mathbf{e}_{tt}(t)\}} = \frac{\omega_c^2}{(s + \omega_c)^2}, \quad (6)$$

$$\frac{\mathcal{L}\{\mathbf{e}_{tt,hf}(t)\}}{\mathcal{L}\{\mathbf{e}_{tt}(t)\}} = \frac{s^2 + 2\omega_c s}{(s + \omega_c)^2}, \quad (7)$$

Table 2: Setup of the end-to-end simulation utilizing the presented control concept (see Section 3.1).

atmosphere	35 layer atmosphere model for average observation conditions at Cerro Armazones
telescope pupil	37 m pupil with 6 equally spaced spiders
guide star & target	point source at the zenith with a wavelength of 2.2 $\mu\text{m}$ and a magnitude of 4.45 mag
active mirrors	<ul style="list-style-type: none"> <li>• M4: <ul style="list-style-type: none"> <li>• 6 segments where the first 300 mechanical modes can be commanded respectively (see Section 2.1)</li> <li>• decoupled temporal dynamics for the mechanical modes according to Eq. (1)</li> <li>• no saturation of actuator strokes</li> </ul> </li> <li>• M5: <ul style="list-style-type: none"> <li>• tip and tilt can be commanded (modal representation, see Section 2.2)</li> <li>• decoupled temporal dynamics for the mechanical modes according to Eq. (2)</li> <li>• no saturation of actuator strokes</li> </ul> </li> </ul>
wavefront sensing	<ul style="list-style-type: none"> <li>• modulated infrared pyramid wavefront sensor</li> <li>• ideal wavefront reconstructor</li> </ul>
SCAO controller	<ul style="list-style-type: none"> <li>• presented control concept (see Fig. 3 and Section 3.1)</li> <li>• crossover network: modified Linkwitz-Riley filters</li> <li>• M4 &amp; M5 controllers: decoupled modal PI controllers</li> <li>• loop frequency = 1 kHz</li> </ul>
simulation tools	COMPASS and MATLAB
time	<ul style="list-style-type: none"> <li>• simulated time = 4 s</li> <li>• time step = 100 <math>\mu\text{s}</math></li> <li>• total time delay = 2 ms (combination of communication and computation delays)</li> </ul>

with the cutoff frequency  $\omega_c = 94.25 \frac{\text{rad}}{\text{s}}$  and the Laplace transform  $\mathcal{L}\{\cdot\}$ . Using these filters guarantees

$$\mathbf{e}_{\text{tt}}(t) = \mathbf{e}_{\text{tt,lf}}(t) + \mathbf{e}_{\text{tt,hf}}(t) \quad \forall t > 0, \quad (8)$$

i. e. no tip-tilt wavefront error is lost or generated by the crossover network. This feature is a significant advantage of the presented crossover network compared to common ones.

## 4.2 Results

To examine the suitability of the presented control concept, the residual wavefront (“behind” the active mirrors) and the applied tip-tilt corrections of the active mirrors were output from the reported end-to-end simulation at a frequency of 1 kHz. Subsequently, the temporal evolution of the residual wavefront and corrections were analyzed.

The temporal evolutions of the short exposure Strehl ratio and the root mean square (rms) value of the residual wavefront in the end-to-end simulation are depicted in Fig. 4. These results show that the Strehl ratio is usually in the range 80...82% with an average of  $\approx 81\%$ . With the given number of M4 modes a maximum Strehl ratio of  $\approx 84\%$  can be achieved. Simulating a modal well-tuned integral controller with a perfect split of the tip-tilt command (mimicking the M4 dynamics, see Eq. (1)) in the same simulation setup, the Strehl ratio is typically in the range 79...81% with an average of  $\approx 80\%$ . Therefore, these results confirm a good wavefront correction despite mirror dynamics, time delays and atmospheric progression via the presented control concept.

Figure 5 presents the temporal evolutions and frequency spectra of the residual wavefront tip and tilt. According to these results, the residual tip and tilt are usually in the range  $\pm 10 \text{ mas}^*$  with rms values of 4.66 mas resp. 4.41 mas. Furthermore, the spectra show no dominant frequencies, especially in the range 10...50 Hz, where

---

\*mas is short for milliarcsecond,  $1 \text{ mas} = 4.848 \cdot 10^{-9} \text{ rad}$

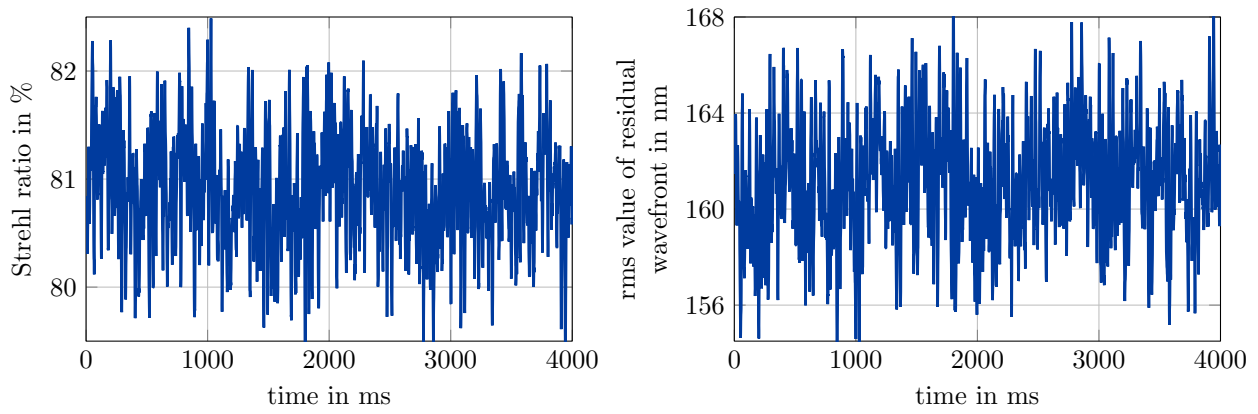


Figure 4: Temporal evolutions of the short exposure Strehl ratio and the rms value of the residual wavefront present in the reported simulation.

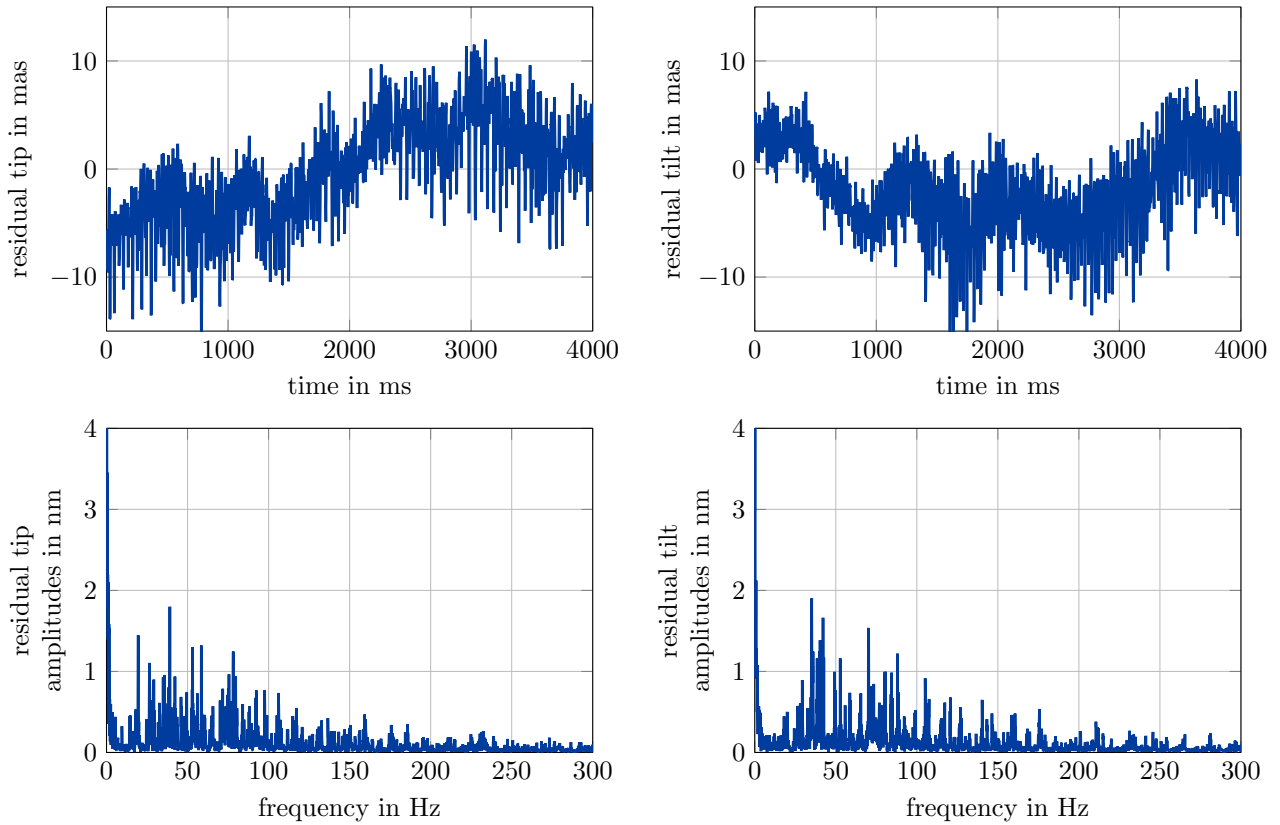


Figure 5: Temporal evolutions and frequency spectra of the residual tip and tilt wavefront in the reported simulation.



the correction of tip and tilt errors switches from the TTM (M5) to the DM (M4). These results support the good correction of wavefront errors by the presented control concept.

The temporal evolutions of M4 resp. M5 tip and tilt in the end-to-end simulation are shown in Fig. 6. This figure indicates that the tip-tilt correction of M4 is usually in the range  $\pm 60$  mas, while the correction of M5 is a few thousand mas. Furthermore, these results confirm the desired tip-tilt split: low-frequency tip-tilt errors are corrected by M5, whereas just high-frequency errors are suppressed by M4.

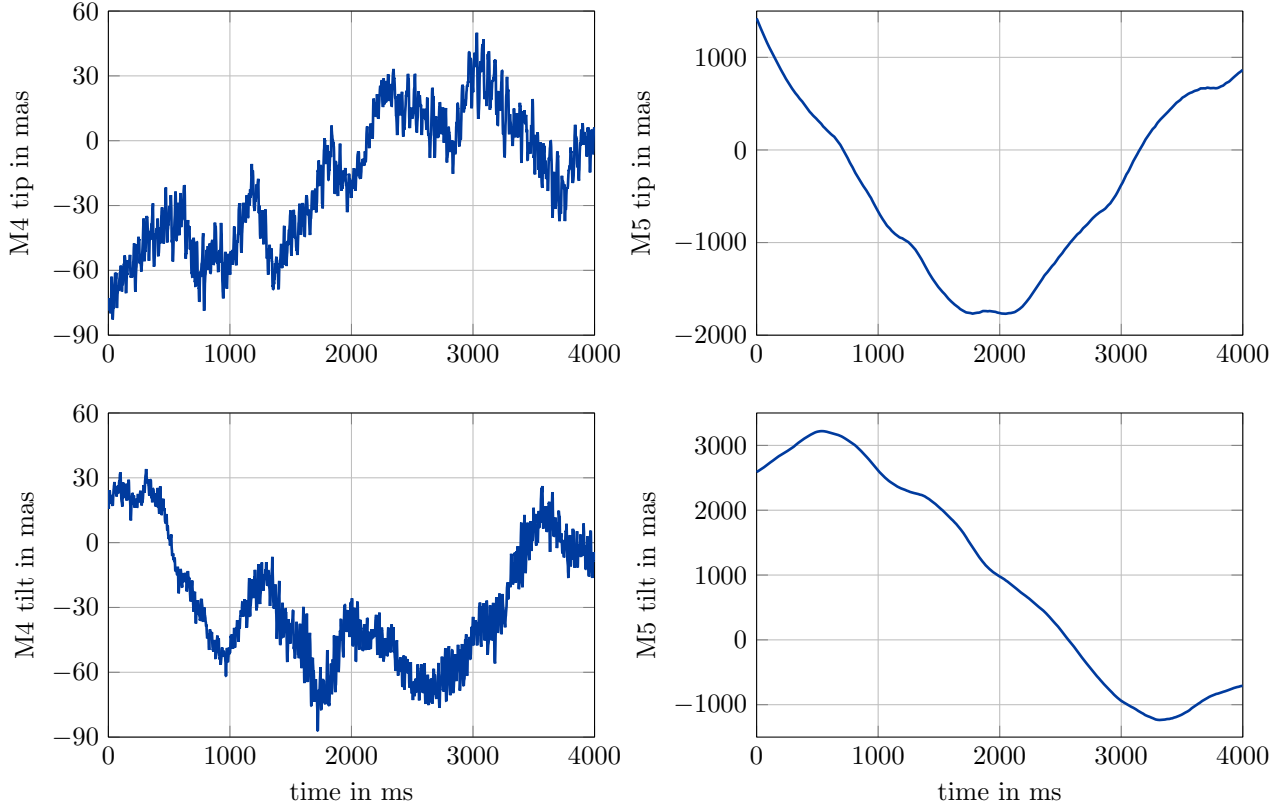


Figure 6: Temporal evolutions of M4 resp. M5 tip and tilt in the reported simulation.

All together, the end-to-end simulation results confirm that the presented modal and model-based control concept corrects the wavefront error well for the complex system configuration of the METIS-SCAO system (dual-stage system, temporal mirror dynamics, ...). In particular, the tip-tilt correction is split properly between M4 and M5. It should be noted that the wavefront correction resp. Strehl ratio obtained via the presented control concept can be improved by using more mechanical M4 modes.

## 5. CONCLUSION

In this article we presented a new model-based control concept relying on the mechanical modes of the active mirrors M4 and M5 for the METIS-SCAO system. The presented concept assigns the temporal low-frequency tip-tilt component of the wavefront error to M5 and the “remaining” wavefront error to M4. Subsequently, two independent controllers command the active mirrors according to the assigned wavefront error components and are based on the mechanical mirror modes. An end-to-end simulation shows that the presented control concept using modal PI controllers suppresses the wavefront error well under METIS-like observation conditions.

The presented control concept splits the tip-tilt correction computationally cheap between the active mirrors based on their dynamics and relieves M4 as far as possible of these corrections. Additionally, the concept can be

easily reconfigured to compensate faulty M4 actuators. Furthermore, the modal mirror controllers can be designed independently and fully customized to the respective mirror. Moreover, the concept can be easily extended to include additional features. Therefore, the application of the presented control in the METIS-SCAO system is very promising.

Based on the presented control concept and simulation results, we will investigate which crossover networks and mirror controllers provide the best wavefront correction for METIS. Furthermore, the control concept will be extended by additional features, e.g. the handling of actuator stroke limitations. Moreover, we will study the modeling of the M4 segment plates more detailed in future publications.

## ACKNOWLEDGMENTS

The authors would like to thank their colleagues at ISYS and MPIA, especially Martin Glück, for their helpful suggestions and comments.

## REFERENCES

- [1] Bertram, T., Bizenberger, P., Briegel, F., Cantalloube, F., Vázquez, M. C. C., Feldt, M., Henning, T., Hippler, S., Huber, A., Mohr, L., Naranjo, V., Rohloff, R.-R., Scheithauer, S., van Boekel, R., Stuik, R., Absil, O., Obereder, A., Glauser, A. M., Hurtado, N., Kulas, M., Kenworthy, M. A., Brandner, W., Carlomagno, B., Neureuther, P., and Shatkhina, I., “Single conjugate adaptive optics for METIS,” in [*Adaptive Optics Systems VI*], Schmidt, D., Schreiber, L., and Close, L. M., eds., **10703**, SPIE (July 2018).
- [2] Cayrel, M., Dierickx, P., Förster, A., Jochum, L., Haupt, C., Müller, M., Derie, F., Pettazzi, L., Lucuix, C., Vernet, E., and Pirard, J.-F., “ESO ELT optomechanics: construction status,” in [*Ground-based and Airborne Telescopes VII*], Gilmozzi, R., Marshall, H. K., and Spyromilio, J., eds., **10700**, SPIE (July 2018).
- [3] Manetti, M., Morandini, M., and Mantegazza, P., “Self-tuning shape control of massively actuated adaptive mirrors,” *IEEE Transactions on Control Systems Technology* **22**, 838–852 (May 2014).
- [4] Barriga, P., Sedghi, B., Dimmler, M., and Kornweibel, N., “Status of E-ELT M5 scale-one demonstrator,” in [*Ground-based and Airborne Telescopes V*], Stepp, L. M., Gilmozzi, R., and Hall, H. J., eds., *Proc. SPIE* **9145**, SPIE (July 2014).
- [5] Conan, R., Bradley, C., Hampton, P., Keskin, O., Hilton, A., and Blain, C., “Distributed modal command for a two-deformable-mirror adaptive optics system,” *Applied Optics* **46**, 4329–4340 (July 2007).
- [6] Kulcsár, C., Raynaud, H.-F., Petit, C., and Conan, J.-M., “Minimum variance control in presence of actuator saturation in adaptive optics,” in [*Adaptive Optics Systems*], Hubin, N., Max, C. E., and Wizinowich, P. L., eds., *Proc. SPIE* **7015**, SPIE (July 2008).
- [7] Correia, C., Raynaud, H.-F., Kulcsár, C., and Conan, J.-M., “Minimum-variance control for woofer-tweeter systems in adaptive optics,” *Journal of the Optical Society of America A* **27**, A133–A144 (Sept. 2010).
- [8] Correia, C. and Véran, J.-P., “Woofer-tweeter temporal correction split in atmospheric adaptive optics,” *Optics Letters* **37**, 3132–3134 (July 2012).
- [9] Lavigne, J.-F. and Véran, J.-P., “Woofer-tweeter control in an adaptive optics system using a fourier reconstructor,” *Journal of the Optical Society of America* **25**, 2271–2279 (Aug. 2008).
- [10] Sedghi, B., Müller, M., Bonnet, H. M., Dimmler, M., and Bauvir, B., “Field stabilization (tip/tilt control) of E-ELT,” in [*Ground-based and Airborne Telescopes III*], Stepp, L. M., Gilmozzi, R., and Hall, H. J., eds., *Proc. SPIE* **7733**, SPIE (July 2010).
- [11] Gavel, D. and Norton, A., “Woofer-tweeter deformable mirror control for closed-loop adaptive optics: theory and practice,” in [*Adaptive Optics Systems IV*], Marchetti, E., Close, L. M., and Véran, J.-P., eds., *Proc. SPIE* **9148**, SPIE (Aug. 2014).
- [12] Perez, J. J., Toussaint, G. J., and Schmidt, J. D., “Adaptive control of woofer-tweeter adaptive optics,” in [*Advanced Wavefront Control: Methods, Devices, and Applications VII*], Carreras, R. A., Rhoadarmer, T. A., and Dayton, D. C., eds., *Proc. SPIE* **7466**, SPIE (Aug. 2009).
- [13] Vernet, E., Cayrel, M., Hubin, N., Biasi, R., Gallieni, D., and Tintori, M., “On the way to build the M4 unit for the E-ELT,” in [*Adaptive Optics Systems IV*], Marchetti, E., Close, L. M., and Véran, J.-P., eds., **9148**, SPIE (July 2014).

- [14] Balas, M. J., “Modal control of certain flexible dynamic systems,” *SIAM Journal on Control and Optimization* **16**, 450–462 (May 1978).
- [15] Ferreira, F., Gratadour, D., Sevin, A., Doucet, N., Gendron, E., Vidal, F., and Deo, V., “Real-time end-to-end AO simulations at ELT scale on multiple GPUs with the COMPASS platform,” in [*Adaptive Optics Systems VI*], Schmidt, D., Schreiber, L., and Close, L. M., eds., *Proc. SPIE* **10703**, SPIE (July 2018).
- [16] Ferreira, F., Gratadour, D., Sevin, A., and Doucet, N., “COMPASS: An efficient GPU-based simulation software for adaptive optics systems,” in [*2018 International Conference on High Performance Computing & Simulation (HPCS)*], 180–187, IEEE (July 2018).
- [17] Linkwitz, S. H., “Active crossover networks for noncoincident drivers,” *Journal of the Audio Engineering Society* **24**, 2–8 (Feb. 1976).